## Description of the three main components of the *Sirex noctilio* invasion model

### Model component 1: simulating new entries

We first built a model component for generating new entries of *S. noctilio* at US and Canadian ports. Prior to its detection in the region, *S. noctilio*, like many other forest insect pests, was regularly intercepted at ports of entry in commodities shipped with solid-wood packing materials or in raw wood products (Hoebeke *et al.*, 2005). In turn, the purpose of this model component was to account for the possibility of human-mediated introductions of *S. noctilio* to locations in North America that were geographically distinct at the time from the existing infested range, yet connected to foreign locations where the pest occurs (and perhaps some of the North American locations) through commodity trade. In subsequent model time steps, these new entries have the opportunity to expand and spread as if they were established populations in the broader landscape.

We constructed the entry component in two steps. First, we estimated the 'total' entry potential of *S. noctilio* into eastern North America via marine ports. We focused on marine ports because the US Department of Agriculture (USDA) Animal and Plant Health Inspection Service (APHIS) PestID database, which documents pest species interceptions at US ports of entry (Haack, 2006), had only reported interceptions of the pest on marine cargo shipments, and not on cargo imported by air or via land border crossings. The total entry potential represents the annual probability that *S. noctilio* will be successfully introduced at one or more marine ports of entry in the study region. We estimated this probability by defining a function, $F(t)$, to describe the yearly flow of marine imports to the USA and Canada through time. To construct $F(t)$, we added data showing the total value of imports (in millions of dollars) to the USA each year (US Census Bureau, 2013) to similar annual import data from Statistics Canada (Statistics Canada, 2012). At the time of our analysis (early 2008), import data were available for both countries through 2007. For simplicity, we assumed that the historical volumes of cargo shipments coming specifically from countries with *S. noctilio* were correlated with the historical trends observed for all marine imports to the USA and Canada.

We next rescaled $F(t)$ to a probability density function, $p(t)$, representing the total probability of successful *S. noctilio* entry into North America. We did this by first defining two points along the $F(t)$ curve: (i) an initial time step, $t_0$; and (ii) the date of the species' first successful introduction, $T_{\text{entry}}$ (see Fig. S13.1). The area under the curve between $t_0$ and $T_{\text{entry}}$ can be set equal to 1, such that:

$$\int_{t_0}^{T_{\text{entry}}} p(t)\,\mathrm{d}t = 1 \tag{S13.1}$$

Subsequently, if $t$ is represented as a discrete annual time step, the value of $p(t)$ can be found by solving Eqn S13.1 numerically:

$$p(t) = \frac{F(t)}{\sum_{t_0}^{T_{\text{entry}}} F(t)} \tag{S13.2}$$

We set $t_0$ to 1971; this was the earliest date for which summary import data were available for both the USA and Canada. We set $T_{\text{entry}}$ to 1999, thereby assuming a 5-year lag between

the entry of *S. noctilio* into North America and its first detection in 2004 (Fig. S13.1). As with many other invasive species, the exact date of the species' entry is unknown, but there is typically a lag of several years between initial arrival of an invader and its detection (Crooks, 2005). We believed an assumption of a 5-year lag was reasonable, but recognize that choosing a different year for $T_{entry}$ would have affected the $p(t)$ values. Notably, Eqn S13.2 can be used to estimate $p(t)$ for values of $t$ that fall outside the bounds of $t_0$ and $T_{entry}$. In this case, it allowed us to estimate $p(t)$ for future years (i.e. after $T_{entry}$ = 1999). However, it also required the simplifying assumption that $F(t)$ in any future year would remain proportional to the sum of $F(t)$ values between $t_0$ and $T_{entry}$. We were comfortable with this assumption given our relatively short time horizon, but acknowledge that this particular solution may be inappropriate for longer time horizons of several decades or more, when individual $F(t)$ values could eventually be several times greater than this sum.

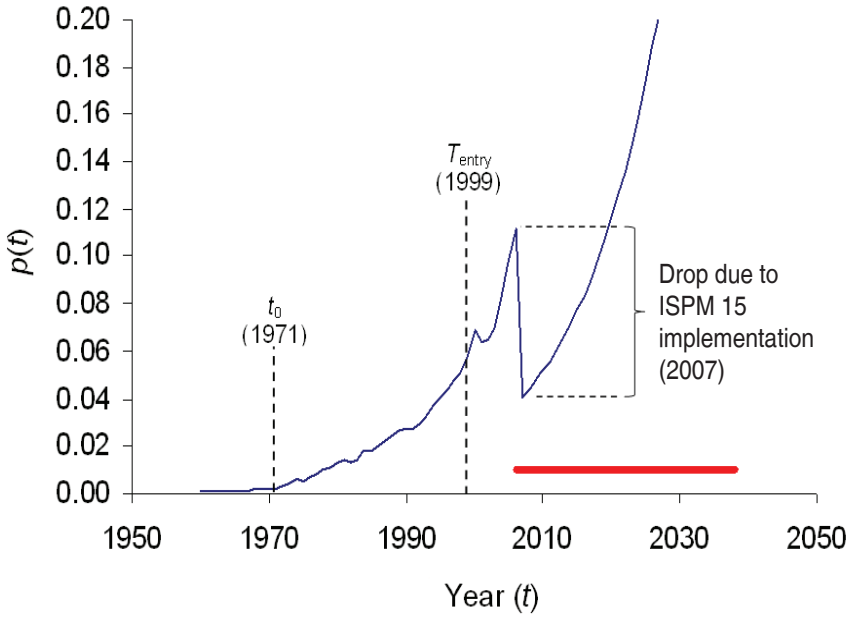


**Fig. S13.1.** Graph of $p(t)$, as calculated from the total value of imports to the USA each year (see Eqns S13.1 and S13.2). The time steps $t_0$ and $T_{entry}$ represent, respectively, the first year in which summary import data were available and the year when *S. noctilio* was assumed to have arrived in the study region (i.e. eastern North America). The red bar indicates the 30-year time horizon, $T$, for the invasion model.

We used Eqn S13.2 as described to estimate $p(t)$ annually through 2006. That year, the USA and Canada fully implemented new phytosanitary standards that had been developed and adopted by the International Plant Protection Convention. Denoted as ISPM 15, these standards for the treatment and handling of all raw wood and wood packing materials were intended to substantially reduce accidental introductions of alien forest pests via imported cargo. We assumed a 50% immediate impact of the new standards on the probability of entry in 2007, supposing that port authorities would increase inspection efforts in order to enforce the new phytosanitary standards. These additional inspections would likely increase the probability of early detection and containment of infested cargoes and therefore reduce the probability of new *S. noctilio* establishments. However, we also assumed the new standards would have a diminishing impact through time because growing import volumes would

begin to outstrip enforcement capacity to some degree. Under this latter assumption, $p(t)$ increases approximately 7% per year after 2007 (see Fig. S13.1). Admittedly, this somewhat pessimistic scenario was conjectural, especially given the impact of the Global Financial Crisis on imports to the USA and Canada in 2008–2009. Nonetheless, more recently available data have shown that US import volumes had already exceeded their pre-Crisis levels by 2010, providing support for our assumption (Williams and Donnelly, 2012).

**Table S13.1.** Commodity categories with the potential to harbour *S. noctilio* either directly (i.e. in raw wood products) or indirectly (i.e. in solid-wood packing materials). Individual commodities were identified by examining historical interception records in the USDA APHIS PestID database. These were then matched to categories in the Lock Performance Monitoring System (PMS), the commodity coding system used by the US Army Corps of Engineers for foreign waterborne commerce statistics.

| Commodity category | PMS commodity code |
|---|---|
| Forest Products, Lumber, Logs, Woodchips | 41 |
| Sand, Gravel, Stone, Rock, Limestone, Soil, Dredged Material | 43 |
| Paper and Allied Products | 51 |
| Building Cement and Concrete, Lime, Glass | 52 |
| Primary Iron and Steel Products (Ingots, Bars, Rods, etc.) | 53 |
| Primary Non-Ferrous Metal Products, Fabricated Metal Products | 54 |
| Primary Wood Products, Veneer, Plywood | 55 |
| All Manufactured Equipment, Machinery and Products | 70 |

After $p(t)$ was estimated out to our model time horizon (i.e. 2036), the next step was to apportion the yearly value of $p(t)$, the total probability of successful *S. noctilio* entry into the study region, among 148 marine ports in the eastern USA and Canada. These ports were identified as principal ports due to their comparatively high shipping volumes (see below). For each time step $t$, we assumed the sum of $W_{x(t)}$, a vector of the local probabilities of *S. noctilio* entry at each individual port $x$, was equal to $p(t)$. To find values of $W_{x(t)}$ in the USA, we used the US Army Corps of Engineers database of foreign cargo shipments to US marine ports (US Army Corps of Engineers Navigation Data Center, 2013). At the time of our analysis, the database reported tonnages of marine imports received between 1997 and 2005, by commodity category and origin country. For Canadian marine ports, we used Statistics Canada 'Shipping in Canada' 2000–2004 reports (Statistics Canada, 2003a,b, 2004, 2005, 2007). The Canadian data provided coarser estimates for major ports only, and over five instead of eight years. Given the available data, we adopted the simplifying assumption that $W_{x(t)}$ follows a linear trend with respect to time. For each port, we determined total annual volumes of commodities that could be infested by *S. noctilio* (Table S13.1) and were imported from countries where it was previously established (Table S13.2). Both the commodity and country lists were assembled by a working group organized by the USDA Forest Service's Forest Health Technology Enterprise Team (FHTET) to develop risk map products for *S. noctilio* (USDA Forest Service Forest Health Technology Enterprise Team, 2013).

**Table S13.2.** List of countries (other than the USA and Canada) where *S. noctilio* is either native or established as an alien species.

| | | | | |
|---|---|---|---|---|
| Albania | Croatia | Ireland | Poland | Spain |
| Argentina | Denmark | Italy | Portugal | Sweden |
| Australia | Estonia | Latvia | Romania | Turkey |
| Belgium | Finland | Lithuania | Russia | Ukraine |
| Brazil | France | Netherlands | Serbia | United Kingdom |
| Bulgaria | Germany | New Zealand | Slovenia | Uruguay |
| Chile | Greece | Norway | South Africa | |

According to the available marine import data, the volumes of *S. noctilio*-associated commodities received at individual US and Canadian ports varied by as much as seven orders of magnitude. We believed this to be an unrealistic characterization of the variability between ports with respect to the local entry probability; we reviewed historical interceptions of *S. noctilio*, other siricids and related insects in the USDA APHIS PestID database and found a much smaller discrepancy (about three orders of magnitude) between the interception frequencies at relatively low-volume ports versus the highest-volume ports. Therefore, we used the following transformation to convert the original cargo volumes into the local entry probability values in $W_{x(t)}$:

$$W_{x(t)} = 10^{-(3/\{1+12\exp[-1.72\log(V_{x(t)})]\})} \tag{S13.3}$$

where $V_{x(t)}$ is the proportion of *S. noctilio*-associated imports that arrived at a particular port $x$ in year $t$. We calculated this proportion as:

$$V_{x(t)} = \frac{v_{x(t)}}{\sum_{x=1}^{Z} v_{x(t)}} \tag{S13.4}$$

where $v_{x(t)}$ is the tonnage of *S. noctilio*-associated cargo (see Tables S13.1 and S13.2) received at $x$ in year $t$ and $Z$ is the total number of ports (i.e. 148). In keeping with our findings from the PestID database, this transformation reduced the variation between ports to roughly three orders of magnitude by shrinking the lower tail of the distribution (i.e. increasing the lowest values) while keeping the upper values unchanged. We then rescaled $W_{x(t)}$ to fit $p(t)$, so:

$$\sum_{x=1}^{Z} W_{x(t)} = p(t) \tag{S13.5}$$

In summary, these equations set the entry potential to a minimum value (0.0008–0.005 per year) for ports with cargo imports below ~$2 \times 10^5$ tonnes per year and then applied the log transform for ports with capacities above ~$2 \times 10^5$ tonnes per year. Note that ports in close proximity (20 km or less) were aggregated to simplify the model calculations.

We used the $W_{x(t)}$ probability values to simulate new entries of *S. noctilio* into eastern North America. We followed the concept, outlined by Rafoss (2003), where discrete stochastic simulation of entry locations is used to predict the establishment potential of an invading organism through time. Before the simulations, the model generated $W_{x(t)}$ for each port of entry for the entire simulation horizon and then recreated the stochastic realization of the entry process for each year. Successful entries were added to a temporary map of known *S. noctilio* locations, which served as a starting point for the simulation of spread and establishment at each time step.

## Model component 2: simulating *S. noctilio* spread

We simulated spread as a travelling wave (Sharov and Liebhold, 1998) in a two-dimensional landscape. Because of the lack of data regarding the dispersal of *S. noctilio* in North America, we relied heavily on expert estimates (Peter de Groot, Canadian Forest Service; Dennis Haugen, USDA Forest Service) when developing this spread function. Much of the experts' knowledge was derived from observations about the species' dispersal behaviour in the southern hemisphere. However, the estimates also incorporate the limited information that could be derived from the recently discovered infestations in Ontario and New York.

Briefly, for any given map cell, the model calculates the colonization rate (i.e. the rate of successful dispersal), $b(d)$, as a function of the distance from the nearest location with an established *S. noctilio* population. The values of $b(d)$ for *S. noctilio* were estimated through consultation with the aforementioned experts and fitted to a distance-decay function:

$$b(d) = p_0 / (1.13 + 0.096d^{1.492}), \text{ for } d < d_{\max} \quad \text{and} \quad b(d) = 0, \text{ for } d \geq d_{\max} \qquad \text{(S13.6)}$$

where $p_0$ is the probability of 'local' dispersal (i.e. the probability of dispersal at a distance of 1 km, corresponding to the spatial resolution at which the model was originally formulated), $d$ is the distance in kilometres from the nearest infested location (measured from the centre of the grid cell) and $d_{\max}$ is the maximum distance at which dispersing *S. noctilio* populations become established. Effectively, $d_{\max}$ describes the flight potential of *S. noctilio* at the population level, although the maximum flight distance for an individual can be considerably higher. We set $d_{\max}$ to 50 km/year and $p_0$ to 0.2, again based on expert consultation. For each year, the model tracks locations with established populations and uses the spread model to disperse *S. noctilio* across the landscape.

The colonization rate is independent of the number of *S. noctilio* individuals at the source location. The spread component of our model operates at a coarse level; in particular, it does not track population numbers, instead assuming that if *S. noctilio* is present in a location, then the population is sufficiently large for the location to serve as a viable dispersal source at the probabilities defined by Eqn S13.6. Nevertheless, any stochastic dispersal function could be substituted for the one we utilized here.

## Model component 3: simulating *S. noctilio* establishment

Dispersing *S. noctilio* individuals do not necessarily translate to established populations. In the model, a few general factors determine the likelihood of successful long-term population establishment in a given map location (i.e. map cell): (i) *S. noctilio* population growth and its constraints; (ii) availability of suitable hosts; and (iii) the susceptibility of the hosts in that location, which depends on both host species and age.

With respect to growth, in a cell successfully invaded by *S. noctilio*, the maximum population size is constrained by a carrying capacity, $k$, which is reached by geometric growth at a constant annual rate, $R$ (Sharov and Liebhold, 1998):

$$N_{j(t+1)} = RN_{j(t)} \ \forall \ N_{j(t+1)} < k \quad \text{and} \quad N_{j(t+1)} = k \ \forall \ N_{j(t+1)} \geq k \qquad \text{(S13.7)}$$

where $N_{j(t)}$ and $N_{j(t+1)}$ are the population densities in the invaded cell at years $t$ and $t + 1$. Essentially, $k$ limits the maximum volume of pine killed by *S. noctilio* at time $t$, $\lambda_{j(t)}$, depending on $\mu$, the minimum volume of pine required to support a single population unit:

$$\lambda_{j(t)} = \mu N_{j(t)} \ \forall \ N_{j(t)} < k \qquad \text{(S13.8)}$$

Because the *S. noctilio* population density in a map cell at any given time *t* may be limited by the amount of currently available (i.e. unconsumed) host resource, the carrying capacity serves as an important constraint that sets the annual limit for host mortality, which in turn affects the establishment potential.

To depict the availability of host resources for *S. noctilio*, we constructed maps of the average age and volume of pine stands, in cubic metres per hectare, for each map cell in the study area. Although numerous data sources (including remotely sensed data) can be utilized to estimate the spatial distributions of forest species, it is difficult to estimate age and volume from such sources. Therefore, we used Canada's National Forest Inventory (CanFI) database to build the Canadian portion and the USDA Forest Service Forest Inventory and Analysis (FIA) database to generate the US portion of the pine map. Details about the designs of these two inventories have been published elsewhere (Gillis *et al.*, 2005; Reams *et al.*, 2005); the US and Canadian databases had fundamentally different structures (i.e. systematic sample plot observations in the US FIA versus area records in the CanFI) that required different spatial interpolation techniques to map pine volumes and average forest stand age at a regional scale. For the US portion, we performed ordinary kriging (Cressie, 1993) of the FIA plot values for these two variables with a spherical semivariogram. The Canadian portion of the map was generated by integrating CanFI data with a satellite-based land-cover classification using spatial randomization techniques (Yemshanov *et al.*, 2012).

**Table S13.3.** Pine (*Pinus*) species growing in the US and/or Canada and documented in the countries' forest inventory data. Ratings of species susceptibility to *S. noctilio* attack (from very high to low) were determined by a working group convened by the Forest Service's Forest Health Technology Enterprise Team.

| Susceptibility rating | Species |
|---|---|
| Very high | Austrian pine (*P. nigra*), Monterey pine (*P. radiata*), Scots pine (*P. sylvestris*), loblolly pine (*P. taeda*) |
| High | Jack pine (*P. banksiana*), lodgepole pine (*P. contorta*), shortleaf pine (*P. echinata*), slash pine (*P. elliottii*), Jeffrey pine (*P. jeffreyi*), ponderosa pine (*P. ponderosa*), red pine (*P. resinosa*), Virginia pine (*P. virginiana*) |
| Medium | Arizona pine (*P. arizonica*), knobcone pine (*P. attenuata*), sand pine (*P. clausa*), Apache pine (*P. engelmannii*), spruce pine (*P. glabra*), bishop pine (*P. muricata*), longleaf pine (*P. palustris*), Table Mountain pine (*P. pungens*), pitch pine (*P. rigida*), pond pine (*P. serotina*), Washoe pine (*P. washoensis*) |
| Low | Whitebark pine (*P. albicaulis*), bristlecone pine (*P. aristata*), foxtail pine (*P. balfouriana*), Mexican pinyon pine (*P. cembroides*), Coulter pine (*P. coulteri*), border pinyon (*P. discolor*), common pinyon (*P. edulis*), limber pine (*P. flexilis*), sugar pine (*P. lambertiana*), Chihuahua pine (*P. leiophylla* var. *chihuahuana*), Great Basin bristlecone pine (*P. longaeva*), singleleaf pinyon (*P. monophylla*), Arizona pinyon pine (*P. monophylla* var. *fallax*), western white pine (*P. monticola*), Parry pinyon pine (*P. quadrifolia*), grey pine (*P. sabiniana*), southwestern white pine (*P. strobiformus*), eastern white pine (*P. strobus*), Torrey pine (*P. torreyana*) |

Maps for individual pine species occurring in the USA and/or Canada were aggregated into two large species groups based on their susceptibility to *S. noctilio* (Table S13.3): (i) a high-hazard group including all species designated as having 'very high' or 'high' susceptibility by the previously mentioned FHTET working group on *S. noctilio*; and (ii) a low-hazard group including species designated as 'medium' or 'low' susceptibility (USDA Forest Service Forest Health Technology Enterprise Team, 2013). The metric of interest for the host maps was the

proportion of the total forest volume represented by pines (i.e. in either the low- or high-hazard group).

The model also required the representation of pine growth over time. We modelled growth rates, $g_v$, for our two hazard groups using normal yield curves, which depict these rates as a function of stand age (in our case, the average stand age in a map cell). For the Canadian portion of the study, we used normal yield equations from Ung *et al.* (2009). These models provide generalized yield curves as a function of two basic climate variables, degree-days and annual precipitation. We used the USDA Forest Service Forest Vegetation Simulator (FVS) to build yield curves for the US portion of the study area (Dixon, 2013). By integrating growth equations for most common tree species with other environmental parameters, FVS predicts stand species composition and associated volumes at user-specified time steps. The FVS has several regional variants that employ distinct, region-specific tree species growth equations. During the modelling process, we applied four regional variants: the Southern, Northeast, Lake States and Central States variants. The final yield curves were aggregated at the province level of the Forest Service's national framework of ecological units, commonly called ecoregions (Cleland *et al.*, 2007). Note that we built idealized normal yield curves that assumed 100% pine stocking.

Finally, we defined host susceptibility, $s_v$, as a species-dependent function of stand age (i.e. the average stand age in a map cell). A cell's $s_v$ value equates to the probability of successful establishment in the cell, but also serves as a modifier for determining what proportion of pines in the cell are susceptible to *S. noctilio*:

$$s_v = 0 \text{ for } a_j < a_0; \quad s_v = s_{\max} \cdot a_j / (a_{\max} - a_0) \text{ for } a_0 < a_j < a_{\max}; \quad s_v = s_{\max} \text{ for } a_j > a_{\max} \qquad \text{(S13.9)}$$

where $a_j$ is the cell's average stand age in years, $a_0$ is the age of stand closure (20 years), $a_{\max}$ is the age when susceptibility reaches its maximum (65 years) and $s_{\max}$ is the maximum susceptibility value for ageing stands. Basically, the $s_v$ value is set to zero when the stand age is less than the typical age of stand closure for pines (20 years) and is maximized when the stand age exceeds 65 years. We employed different maximum susceptibility values for our two pine groups, assuming $s_{\max}$ = 0.95 for species in the high-hazard group and $s_{\max}$ = 0.50 for species in the low-hazard group (see Table S13.3). Because $s_v$ defines the proportion of susceptible pines in a cell, it combines with host volume to dictate $k$.

With respect to spatial data (i.e. the maps of pine volume and stand age), our model required raster data sets in binary floating-point format (*.flt files, with accompanying header and map projection files). Binary floating-point files can be generated straightforwardly via export from ESRI ArcInfo grid format. Other raster data sets required for the model were an area of interest mask and a raster representation of initial infestations at $t$ = 0 (i.e. map cells where the pest was currently established at the beginning of the simulation runs). The carrying capacity, $k$, was incorporated as a single value, while $s_v$ and $g_v$ were both functions implemented as tables of values at different ages for our two hazard groups.

## References


Cleland, D.T., Freeouf, J.A., Keys, J.E. Jr, Nowacki, G.J., Carpenter, C.A. and McNab, W.H. (2007) *Ecological Subregions: Sections and Subsections for the Conterminous United States. General Techical Report No. WO-76.* Sloan, A.M. (tech. ed.). Map, presentation scale 1:3,500,000, Albers equal area projection. USDA Forest Service, Washington, DC.

Cressie, N.A.C. (1993) *Statistics for Spatial Data*. Wiley, New York.

Crooks, J.A. (2005) Lag times and exotic species: the ecology and management of biological invasions in slow-motion. *Ecoscience* 12, 316–329.

Dixon, G.E. (2013) *Essential FVS: A User's Guide to the Forest Vegetation Simulator, Revised Edition.* USDA Forest Service, Forest Management Service Center, Fort Collins, Colorado.

Gillis, M.D., Omule, A.Y. and Brierley, T. (2005) Monitoring Canada's forests: the National Forest Inventory. *The Forestry Chronicle* 81, 214–221.

Haack, R.A. (2006) Exotic bark- and wood-boring Coleoptera in the United States: recent establishments and interceptions. *Canadian Journal of Forest Research* 36, 269–288.

Hoebeke, E.R., Haugen, D.A. and Haack, R.A. (2005) *Sirex noctilio*: discovery of a palearctic siricid woodwasp in New York. *Newsletter of the Michigan Entomological Society* 50, 24–25.

Rafoss, T. (2003) Spatial stochastic simulation offers potential as a quantitative method for pest risk analysis. *Risk Analysis* 23, 651–661.

Reams, G.A., Smith, W.D., Hansen, M.H., Bechtold, W.A., Roesch, F.A. and Moisen, G.G. (2005) The Forest Inventory and Analysis sampling frame. In: Bechtold, W.A. and Patterson, P.L. (eds) *The Enhanced Forest Inventory and Analysis Program – National Sampling Design and Estimation Procedures. General Technical Report No. SRS-80*. USDA Forest Service, Southern Research Station, Asheville, North Carolina, pp. 11–26.

Sharov, A.A. and Liebhold, A.M. (1998) Model of slowing the spread of gypsy moth (Lepidoptera: Lymantriidae) with a barrier zone. *Ecological Applications* 8, 1170–1179.

Statistics Canada (2003a) *Shipping in Canada 2000. Catalogue No. 54-205-XIE*. Statistics Canada, Ottawa. Available at: http://www.statcan.gc.ca/pub/54-205-x/54-205-x2000000-eng.pdf (accessed 3 January 2014).

Statistics Canada (2003b) *Shipping in Canada 2001. Catalogue No. 54-205-XIE*. Statistics Canada, Ottawa. Available at http://www.statcan.gc.ca/pub/54-205-x/54-205-x2001000-eng.pdf (accessed 3 January 2014).

Statistics Canada (2004) *Shipping in Canada 2002. Catalogue No. 54-205-XIE*. Statistics Canada, Ottawa. Available at: http://www.statcan.gc.ca/pub/54-205-x/54-205-x2002000-eng.pdf (accessed 3 January 2014).

Statistics Canada (2005) *Shipping in Canada 2003. Catalogue No. 54-205-XIE*. Statistics Canada, Ottawa. Available at: http://www.statcan.gc.ca/pub/54-205-x/54-205-x2003000-eng.pdf. (accessed 3 January 2014).

Statistics Canada (2007) *Shipping in Canada 2004. Catalogue No. 54-205-XIE*. Statistics Canada, Ottawa. Available at: http://www.statcan.gc.ca/pub/54-205-x/54-205-x2004000-eng.pdf (accessed 3 January 2014).

Statistics Canada (2012) *Merchandise Imports and Exports, by Major Groups and Principal Trading Areas for all Countries, Annual (Dollars). CANSIM Database Table No. 228-0003*. Statistics Canada, Ottawa. Available at: http://www5.statcan.gc.ca/cansim/a26?lang=eng&retrLang=eng&id=2280003&paSer=&pattern=&stByVal=1&p1=1&p2=-1&tabMode=dataTable&csid= (accessed 3 January 2014).

Ung, C.-H., Bernier, P.Y., Guo, X.J. and Lambert, M.-C. (2009) A simple growth and yield model for assessing changes in standing volume across Canada's forests. *The Forestry Chronicle* 85, 57–64.

US Army Corps of Engineers Navigation Data Center (2013) *US Waterway Data, Foreign Cargo Inbound and Outbound*. US Army Corps of Engineers, Navigation Data Center, Waterborne Commerce Statistics Center, New Orleans, Louisiana. Available at: http://www.navigationdatacenter.us/data/dataimex.htm (accessed 3 January 2014).

US Census Bureau (2013) *US Trade in Goods – Balance of Payments (BOP) Basis vs. Census Basis*. US Census Bureau, Foreign Trade Division, Washington, DC. Available at: http://www.census.gov/foreign-trade/statistics/historical/goods.txt (accessed 3 January 2014).

USDA Forest Service Forest Health Technology Enterprise Team (2013) *Invasive Pest Risk Maps – Sirex Woodwasp –* Sirex noctilio. USDA Forest Service, FHP/FHTET, Fort Collins, Colorado. Available at http://www.fs.fed.us/foresthealth/technology/invasives_sirexnoctilio_riskmaps.shtml (accessed 3 January 2014).

Williams, B.R. and Donnelly, J.M. (2012) *US International Trade: Trends and Forecasts, October 19, 2012.* US Congressional Research Service, Washington, DC.

Yemshanov, D., McKenney, D.W. and Pedlar, J.H. (2012) Mapping forest composition from the Canadian National Inventory and land cover classification maps. *Environmental Monitoring and Assessment* 184, 4655–4669.